
[View Journal Online](#)
[View Article Online](#)

The crystal magnification, characterization, X-ray single crystal structure, thermal behavior, and computational studies of the 2,4,6-trimethylpyridinium picrate

 Nahide Burcu Arslan ¹ and Fatma Aydin ^{2,*}
¹ Department of Computer Education and Instructional Technology, Faculty of Education, Giresun University, 28200, Giresun, Turkey

² Department of Chemistry, Faculty of Arts and Sciences, Canakkale Onsekiz Mart University, 17100, Canakkale, Turkey

 * Corresponding author at: Department of Chemistry, Faculty of Arts and Sciences, Canakkale Onsekiz Mart University, 17100, Canakkale, Turkey.
 e-mail: faydin@comu.edu.tr (F. Aydin).

RESEARCH ARTICLE

ABSTRACT



doi: 10.5155/eurjchem.13.4.468-477.2349

Received: 23 September 2022

Received in revised form: 06 October 2022

Accepted: 24 October 2022

Published online: 31 December 2022

Printed: 31 December 2022

KEYWORDS

 Picric acid
 2,4,6-Collidine
 Thermal properties
 X-ray structure determination
 Molecular electrostatic potential
 2,4,6-Trimethylpyridinium picrate

A crystal of organic salt, 2,4,6-trimethylpyridinium picrate (TMPPc), was synthesized and magnified by slow evaporation in a polar aprotic solvent and characterized by ¹H NMR, ¹³C NMR, and FT-IR spectroscopic methods. X-ray diffraction analysis of the crystal structure of the compound TMPPc showed the presence of a monoclinic space group with $a = 4.0174(4) \text{ \AA}$, $b = 27.863(3) \text{ \AA}$, $c = 13.9247(17) \text{ \AA}$, $\beta = 95.741(4)^\circ$, $V = 1550.9(3) \text{ \AA}^3$, $Z = 4$, $T = 296 \text{ K}$, $\mu(\text{MoK}\alpha) = 0.123 \text{ mm}^{-1}$, $D_{\text{calc}} = 1.500 \text{ g/cm}^3$, 62749 reflections measured ($5.88^\circ \leq 2\theta \leq 57.058^\circ$), 3911 unique ($R_{\text{int}} = 0.0536$, $R_{\text{sigma}} = 0.0226$) which were used in all calculations. The final R_1 was 0.0569 ($I > 2\sigma(I)$) and wR_2 was 0.1710 (all data). Detailed investigation of molecular packing of the TMPPc molecule indicated the presence of intermolecular hydrogen bond between N4-H44...O1 and C13-H13B...O4 that generates $C_2^2(14)$ chain running parallel to the [001] direction. The infrared and Raman spectra of the prepared TMPPc compound were recorded and discussed. The thermal stability of the obtained TMPPc crystal was analysed by TGA/DTG technique and revealed that the crystal was stable up to 162 °C. Density functional theory calculations such as the value of the HOMO and LUMO energy gap, the parameters of the molecular electrostatic potential, the global reactivity and thermodynamic properties of the compound TMPPc were also performed using the DFT/B3LYP method with the level of the 6-311G (d, p) basis set.

 Cite this: *Eur. J. Chem.* 2022, 13(4), 468-477

 Journal website: www.eurjchem.com

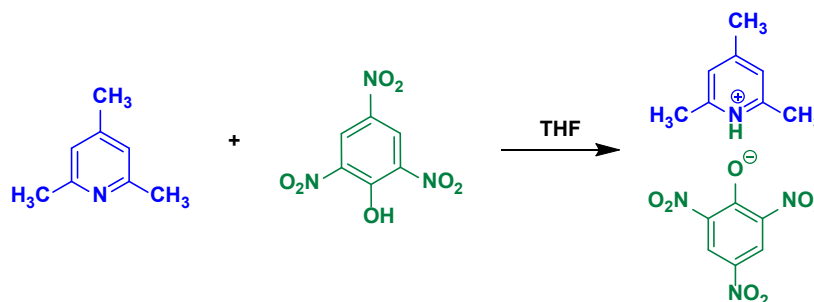
1. Introduction

2,4,6-Trimethylpyridine, as named 2,4,6-collidine, is a pyridine derivative containing three methyl groups. It is useful as a base for a variety of reactions, such as dehydrohalogenation reactions [1]. Besides, it is a sterically hindered base ($pK_a = 7.43$) and is also used as solvent in direct tritylation reactions of weakly acidic compounds as acetone and acetonitrile. It is used as the fluorinating reagent for organo-transition metal alkyls via 2,4,6-trimethyl-pyridine-bis-hydrofluoride [2], as also the electrophilic N-F reagents in the preparations of the pharmaceuticals containing fluoro-aliphatic, aromatic and heterocyclic units [3,4]. It is also important for the synthesis of the bis(2,4,6-trimethyl-pyridine)iodine hexafluorophosphate and bis(2,4,6-trimethyl-pyridine)bromine hexafluorophosphate reagents [5,6].

On another hand, picric acid (PA), as known as 2,4,6-trinitrophenol (TNP), is a phenol derivative containing three nitro groups and has the great possibility of resonance between the nitro groups with the negative charge of phenolic oxygen, thus it is really one of the strongest organic acids ($pK_a = 0.38$) [7]. For organic nonlinear optics (NLO) materials, picric acid is known as an acidic ligand because it tends to form salts,

particularly with aromatic or aliphatic amines [8-11]. Picric acid has been shown to act as an acceptor to form various π -stacking complexes with some aromatic molecules. It has been observed that it can form charge transfer complexes with some aromatic hydrocarbon groups, such as naphthalene, anthracene, etc. [12-14]. In addition, picric acid is widely used in micro dye reactions, in the manufacture of matches, electric batteries, colored glass, disinfectants, and explosives as a component of rocket fuel [15,16]. Moreover, it has been widely used in leathers, pharmaceuticals, agriculture, etc. [17].

Previously, the crystal structure of picrates of various pyridine derivatives were synthesized and grouped, and the geometry and possible H-bond correlations of the pyridinium-picric acid ion pair were investigated [18]. In this study, one of these compounds was examined in more detail and a new perspective was tried to be created for such compounds. Therefore, 2,4,6-trimethylpyridinium picrate was resynthesized, its single crystal was magnified by slow evaporation in THF solvent and characterized by elemental analysis, FT-IR, ¹H NMR, and ¹³C NMR techniques. Its crystal properties were investigated by X-ray diffraction analysis.



Scheme 1. Synthesis pathway of the 2,4,6-trimethylpyridinium picrate.

The optimized molecular geometry, the molecular electrostatic potential (MEP) map, the highest occupied molecular orbital energy (HOMO), the lowest unoccupied molecular orbital energy (LUMO) and the thermodynamic properties were calculated by using density functional theory (DFT) at the B3LYP/6-311G(d,p) level. UV-Visible, infrared, and Raman spectra were recorded and discussed in detail. The thermal behavior of the organic TMPPc salt was also investigated by thermogravimetric analysis (TG/DTG).

2. Experimental

2.1. Material and methods

2,4,6-Trinitrophenol (picric acid), 2,4,6-trimethylpyridine (2,4,6-collidine), ethanol and tetrahydrofuran were purchased from Sigma-Aldrich and Merck Chemical Company. The melting point of the title compound was determined on the Electrothermal 9100[®] apparatus. FT-IR analysis was performed using a PerkinElmer Spectrum-100 FT-IR instrument with an ATR apparatus in the range 4000-650 cm^{-1} . The Raman spectrum was recorded in the region of 3500-150 cm^{-1} on a WitecAlpha 300RA FT-Raman spectrometer by using a 532 nm green laser. The ^1H NMR and ^{13}C NMR spectra were recorded on a JEOL ECX-400 FT-NMR spectrometer operating at 400 and 100 MHz, respectively, using TMS as an internal standard and $\text{DMSO-}d_6$ as solvent. UV-Vis measurements were carried out with a Perkin Elmer WinLab-25 series spectrophotometer in quartz cells of 1 cm path length. The crystal structure analysis of the title compound was carried out using a Bruker APEX-II CCD X-ray diffractometer (MoK α radiation, 0.71073 Å). PerkinElmer TGA 8000 was used for the TG/DTG analysis of the title compound. The 8.60 mg sample was heated at 10 $^\circ\text{C}/\text{min}$ from 30 to 800 $^\circ\text{C}$ in a nitrogen atmosphere.

2.2. The synthesis of the 2,4,6-trimethylpyridinium picrate

Picric acid (moistened with H_2O , $\geq 98\%$, Sigma-Aldrich) was dried over two days at room temperature and recrystallized in ethanol, (Note: Aqueous solution of picric acid was purchased due to the explosive nature of it). Crystallized picric acid (1.145 g, 5 mmol) was dissolved in dry tetrahydrofuran (20 mL) and 2,4,6-trimethylpyridine (0.605 g, 5 mmol) was dropped to the above solution. The mixture was refluxed with stirring for 30 min. After then, the obtained yellow precipitate was filtered by using Whatman filter paper and dried in a vacuum desiccator. The obtained product (picrate salt) was crystallized by slow evaporation from THF as a solvent (Scheme 1).

2,4,6-Trimethylpyridinium picrate (TMPPc): M.p.: 159-160 $^\circ\text{C}$. FT-IR (ATR, ν , cm^{-1}): 3281, 3067, 2921, 2792, 2721, 1612, 1556, 1481, 1329, 1259, 1151, 908, 709. ^1H NMR (400 MHz, $\text{DMSO-}d_6$, δ , ppm): 2.57 (s, 3H, CH_3), 3.29 (s, 6H, CH_3), 7.52 (s, 2H, P ry-H), 8.54 (s, 2H, Ph-H). ^{13}C NMR (100 MHz, $\text{DMSO-}d_6$, δ , ppm): 161.38 (1C, C₆), 159.16 (1C, C₉), 152.34 (2C, C₇, C₁₁),

142.33 (2C, C₂, C₄), 125.68 (2C, C₈, C₁₀), 125.57 (1C, C₉), 124.68 (2C, C₁, C₅), 21.83 (2C, C₁₂, C₁₄), 19.38 (1C, C₁₃).

2.3. X-ray crystallography

A single crystal of 2,4,6-trimethylpyridinium picrate was grown by slow evaporation of the solution of product in tetrahydrofuran. The diffraction data of it were collected on a Bruker APEX-II CCD diffractometer using MoK α radiation. The cell parameters and crystal structure were solved and refined by SHELXS-97 and SHELXL-97 programs, respectively [19,20]. The refinement was carried out by the full-matrix least-squares method on the positional and anisotropic temperature parameters of the non-hydrogen atoms, or equivalently corresponding to 227 crystallographic parameters. The atomic numbering scheme with displacement ellipsoids of the crystal structure drawn with ORTEP-III was depicted at the 30% probability level for clarity (Figure 1). The details of crystal data, experimental condition and structural refinement are listed in Table 1.

2.4. Computational studies

The molecular structure of 2,4,6-trimethylpyridinium picrate was optimized using DFT in the ground state by the B3LYP method with the 6-311G(d,p) basis sets included in Gaussian 09 program [21]. The molecular structure of the salt optimized by 6-311G(d,p) basis set displayed frontier molecular orbitals, and the electrostatic potential was simulated. The frontier molecular orbital and energy gap between the highest occupied and the lowest unoccupied molecular orbitals were calculated with density functional theory. In addition, thermodynamic parameters (*i.e.*, heat capacity, enthalpy, and entropy values) for the title molecule were also calculated.

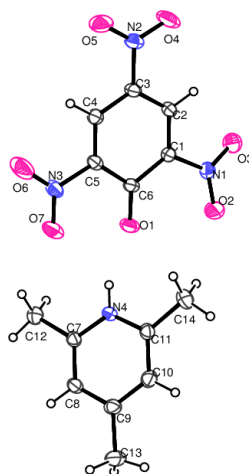
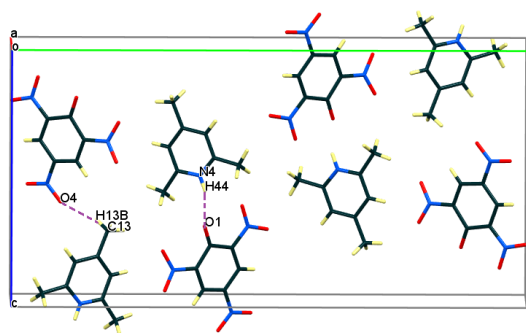
3. Results and discussion

3.1. Crystal structure and optimized geometry

The 2,4,6-trimethylpyridinium picrate crystal, magnified by slow evaporation in a polar aprotic solvent (THF), is in the monoclinic form with space group $P2_1/c$ with $Z = 4$ in the unit cell, similar to the literature [18]. The title compound consists of the 2,4,6-trimethylpyridinium and 2,4,6-trinitrophenolate moieties. The molecular packing diagram of the prepared compound is located along the a -axis (Figure 2). Due to the functional groups of the compound, the b -axis and the c -axis 27.863(3) and 13.9247(17) Å, respectively, are larger than the a -axis 4.0174(4) Å in the crystal dimensions. Crystallographic data and details of the X-ray diffraction study of the title compound are shown in Table 1. The bond lengths and bond angles of the 2,4,6-trimethylpyridinium picrate are given in Table 2, while the hydrogen bond details are compiled in Table 3.

Table 1. Crystal data, details of the structure refinement parameters for the 2,4,6-trimethylpyridinium picrate.

Empirical formula	C ₁₄ H ₁₄ N ₄ O ₇
Formula weight	350.29
Temperature (K)	293(2)
Crystal system	Monoclinic
Space group	P2 ₁ /c
<i>a</i> , (Å)	4.0174(4)
<i>b</i> , (Å)	27.863(3)
<i>c</i> , (Å)	13.9247(17)
β (°)	95.741(4)
Volume (Å ³)	1550.9(3)
<i>Z</i>	4
ρ _{calc} (g/cm ³)	1.500
μ (mm ⁻¹)	0.123
F(000)	728.0
Crystal size (mm ³)	0.18 × 0.15 × 0.13
Radiation	MoKα (λ = 0.71073)
2θ range for data collection (°)	5.88 to 57.058
Index ranges	-5 ≤ <i>h</i> ≤ 5, -37 ≤ <i>k</i> ≤ 37, -18 ≤ <i>l</i> ≤ 18
Reflections collected	62749
Independent reflections	3911 [R _{int} = 0.0536, R _{sigma} = 0.0226]
Data/restraints/parameters	3911/0/227
Goodness-of-fit on F ²	1.063
Final R indexes [I ≥ 2σ (I)]	R ₁ = 0.0569, wR ₂ = 0.1513
Final R indexes [all data]	R ₁ = 0.0816, wR ₂ = 0.1710
Largest diff. peak/hole (e.Å ⁻³)	0.33/-0.29
Computer programs	BrukerAPEX2, BrukerSAINT, SHELXT 2014/4, SHELXL2016/6

**Figure 1.** ORTEP III diagram of the 2,4,6-trimethylpyridinium picrate.**Figure 2.** Molecular packing diagram of the 2,4,6-trimethylpyridinium picrate is displaced along the *a*-axis.

The 2,4,6-trinitrophenolate moiety of the compound has a closely planar configuration and the maximum deviation from the mean plane belongs to the O2 oxygen atom with 0.288 Å. The picrate group twists slightly due to the consistency of the trimethyl group. The torsion angle values about this twist are -16.3(3)° on the C6/C1/N1/O2 atom group and 164.98(19)° on the C6/C1/N1/O3 atom group. The molecular packing of the crystal consists of an N-H...O type intramolecular hydrogen bonding and a weak C-H...O interaction. The N2-H2...O1

intramolecular hydrogen bonding occurs between the N2 atom of the 2,4,6-trinitrophenolate group and the O1 atom of the 2,4,6-trimethylpyridinium group with 2.776(2) Å distance of D...A. The C13-H13B and N4-H44 groups in the molecule act as hydrogen-bond donors to atoms O4^{*i*} and O1, respectively (Symmetry code, *i*: *x*, *y*, *z*+1.) forming a C₂²(14) chains running parallel to the [001] direction (Figure 2).

Table 2. Comparison of the optimized and calculated geometry (bond lengths (Å) and bond angles (°) of the 2,4,6-trimethylpyridinium picrate.

Parameters	Experimental	Calculated B3LYP/6-311G(d,p)	Parameters	Experimental	Calculated B3LYP/6-311G(d,p)
Bond lengths (Å)					
C1-C2	1.369(3)	1.3836	C8-C9	1.388(3)	1.3967
C1-C6	1.455(3)	1.4529	C9-C10	1.393(3)	1.3990
C1-N1	1.457(3)	1.4554	C9-C13	1.497(3)	1.5039
C2-C3	1.378(3)	1.3865	C10-C11	1.375(3)	1.3858
C3-C4	1.389(3)	1.3959	C11-N4	1.354(3)	1.3508
C3-N2	1.449(3)	1.4601	C11-C14	1.492(3)	1.4966
C4-C5	1.367(3)	1.3740	N1-O2	1.215(3)	1.2356
C5-C6	1.461(3)	1.4518	N1-O3	1.223(3)	1.2249
C5-N3	1.465(3)	1.4692	N2-O5	1.209(3)	1.2268
C6-O1	1.252(2)	1.2538	N2-O4	1.220(3)	1.2268
C7-N4	1.354(3)	1.3499	N3-O6	1.199(3)	1.2251
C7-C8	1.376(3)	1.3882	N3-O7	1.203(3)	1.2257
C7-C12	1.492(3)	1.4968			
Bond angles (°)					
C2-C1-C6	123.92(19)	123.4756	C8-C9-C10	118.2(2)	118.1433
C2-C1-N1	115.61(18)	116.5486	C8-C9-C13	121.5(2)	121.1031
C6-C1-N1	120.47(18)	119.9489	C10-C9-C13	120.3(2)	120.7460
C1-C2-C3	120.12(19)	119.6391	C11-C10-C9	121.0(2)	120.5834
C2-C3-C4	120.89(19)	120.8270	N4-C11-C10	118.09(19)	118.4516
C2-C3-N2	119.69(19)	119.5960	N4-C11-C14	118.1(2)	117.3962
C4-C3-N2	119.4(2)	119.5748	C10-C11-C14	123.8(2)	124.1487
C5-C4-C3	119.0(2)	119.3309	O2-N1-O3	121.2(2)	123.3341
C4-C5-C6	124.73(19)	124.0346	O2-N1-C1	120.1(2)	118.1011
C4-C5-N3	115.56(19)	116.7237	O3-N1-C1	118.6(19)	118.5569
C6-C5-N3	119.71(18)	119.2403	O5-N2-O4	122.6(2)	124.6459
O1-C6-C1	124.1(2)	125.3451	O5-N2-C3	119.2(2)	117.6111
O1-C6-C5	124.60(19)	122.0752	O4-N2-C3	118.2(2)	117.7428
C1-C6-C5	111.28(17)	112.4751	O6-N3-O7	120.7(2)	124.3083
N4-C7-C8	118.28(19)	118.3672	O6-N3-C5	118.3(2)	117.4655
N4-C7-C12	118.57(19)	117.5172	O7-N3-C5	121.0(2)	118.1909
C8-C7-C12	123.1(2)	124.1106	C11-N4-C7	123.61(18)	123.8217
C7-C8-C9	120.8(2)	120.6323			

Table 3. Hydrogen-bond geometry (Å, °) for the 2,4,6-trimethylpyridinium picrate.

D-H...A	D-H	H...A	D...A	∠ D-H...A
N4-H44...O1	0.86	1.96	2.776 (2)	159
C13-H13B...O4 ⁱ	0.96	2.30	3.233 (4)	163

Symmetry code: (i) x, y, z+1.

The formation of salt appears due to intramolecular proton transfer from the oxygen atom in 2,4,6-trinitrophenol to the nitrogen atom in 2,4,6-trimethylpyridine.

The optimized geometry parameters (theoretical) for the title compound, namely, the bond lengths and bond angles, were calculated using the B3LYP/6-311G(d,p) method and are listed in Table 2. The correlation coefficient data between the calculated and experimental geometrical parameters (bond length and bond angle values) were calculated. The data obtained show that almost all optimized bond lengths and bond angles are slightly larger than the experimental values. The correlation coefficient values for the bond length and bond angles by experimental and theoretical (B3LYP) are 0.9944 and 0.8043, respectively.

The molecular conformation described by the torsional angles obtained from the X-ray data is C1-C2-C3-N2 and N3-C5-C6-C1 178.8(2)°, -179.19288° and -177.65(18)°, 175.0860°, as obtained by the experimental method, are smaller than those determined by the B3LYP method, as observed in the reported research paper [22].

3.2. ¹H NMR and ¹³C NMR analysis

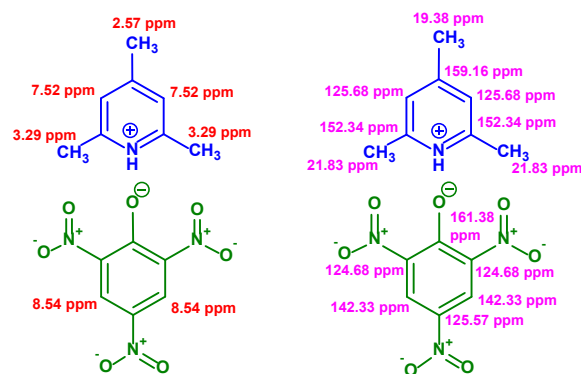
The ¹H and ¹³C NMR spectrum of 2,4,6-trimethylpyridinium picrate is obtained in DMSO-*d*₆. The OH proton signal in free picric acid normally appears at δ 11.94 ppm [23]. There is no OH signal observed in the ¹H NMR spectrum due to the migration of the phenolic proton to pyridine nitrogen during the formation of TMPPC. The singlet peak at δ 8.54 ppm is assigned to the protons of the aromatic carbon atoms (C2 and C4) in the picrate moiety. The singlet peak at δ 7.52 ppm is due to the protons at C8 and C10 carbons of the pyridinium moiety. The presence of two different methyl protons at δ 3.29 (s, 6H)

and 2.57 ppm (s, 3H) is confirmed by the appearance of the signals of the cationic moiety as 2,4,6-trimethylpyridinium.

In the ¹³C NMR spectra of the title compound, there are magnetically and chemically two different aromatic rings. The ipso carbon (C6) signal of the picrate group appears at δ 161.29 ppm. The observed peaks at δ 142.33 and 125.57 ppm of the crystal were due to *ortho* (C1-C5) and *para* (C3) carbon atoms that contain the NO₂ group in the picrate moiety, respectively. The peak at δ 124.68 ppm is assigned to the *meta* carbons (C2 and C4) of the picrate moiety. The observed peaks at δ 159.16 and 152.34 ppm of the crystal were due to C7-C11 and C9 carbon atoms containing CH₃ group in the pyridinium moiety, respectively. The peak at δ 125.68 ppm is assigned to the C8 and C10 carbons of the picrate moiety. The methyl groups in the structure of the pyridinium picrate derivatives were confirmed at δ 21.83 and 19.38 ppm, respectively (Scheme 2).

3.3. FT-IR and Raman spectroscopic analysis

FT-IR spectra of the 2,4,6-trimethylpyridine, picric acid, and 2,4,6-trimethylpyridinium picrate are given in Figure 3. In the split spectrum, while some functional groups are disappeared, some functional groups are appeared due to picrate salts. In the FT-IR spectrum, the broad peak observed at 3274 cm⁻¹ is assigned to the presence of a hydrogen-bonded phenolic group [24]. The FT-Raman spectrum of 2,4,6-trimethylpyridinium picrate is also shown in Figure 4. In the Raman spectrum, this phenolic group peak does not appear to be very pronounced. The C-H vibrations cover the asymmetric and symmetric stretching vibration modes of the benzene and pyridine rings, as well as the methyl group.



Scheme 2. ^1H and ^{13}C NMR chemical shifts of 2,4,6-trimethylpyridinium picrate in $\text{DMSO-}d_6$.

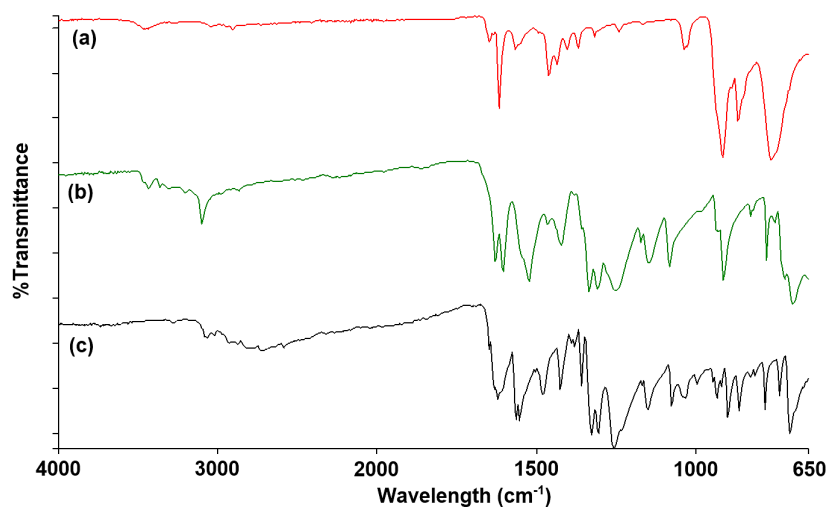


Figure 3. FT-IR spectra of 2,4,6-trimethylpyridine (a), 2,4,6-trinitrophenol (b) and 2,4,6-trimethylpyridinium picrate (c).

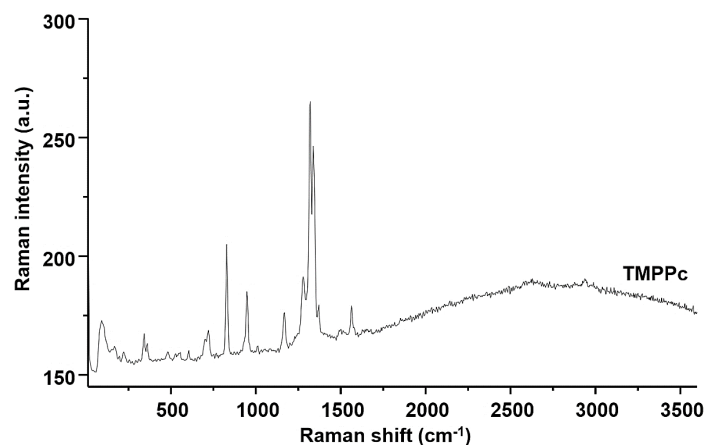


Figure 4. Raman spectrum of the 2,4,6-trimethylpyridinium picrate.

Vibration bands at 3068 and 3027 cm^{-1} ($\nu_{\text{C-H}}$), 1566 and 1556 cm^{-1} ($\nu_{\text{C=Carom}}$) in FT-IR spectra were observed as the result of the vibration of pyridyl and phenyl rings, respectively.

Asymmetric and symmetric stretching vibrations of aliphatic C-H bonds of methyl groups normally appear in the range of 3000 - 2700 cm^{-1} [25]. There are two different methyl functional groups ($-\text{CH}_3$) attached to the aromatic ring in the structure of the crystal molecule. The peaks observed at 2934 , 2872 , and 2723 cm^{-1} in FT-IR spectra and 2933 , 2817 and 2762 cm^{-1} in Raman spectra, respectively, confirm the existence of

aliphatic C-H stretching vibrations of the TMPPc compound. Strong C-H bending vibrations are also observed at 904 and 913 cm^{-1} in the FT-IR and the Raman spectra, respectively. Furthermore, the peaks occurring at 1622 and 1648 cm^{-1} are defined as the C=N stretching vibrations of TMPPc in the FT-IR and Raman spectra, respectively, and are attributed to the presence of the pyridinium core. The absorption bands at 1481 and 1258 , 1454 and 1272 cm^{-1} are assigned to C-C and C-N stretching vibrations in FT-IR and Raman spectra, respectively [26].

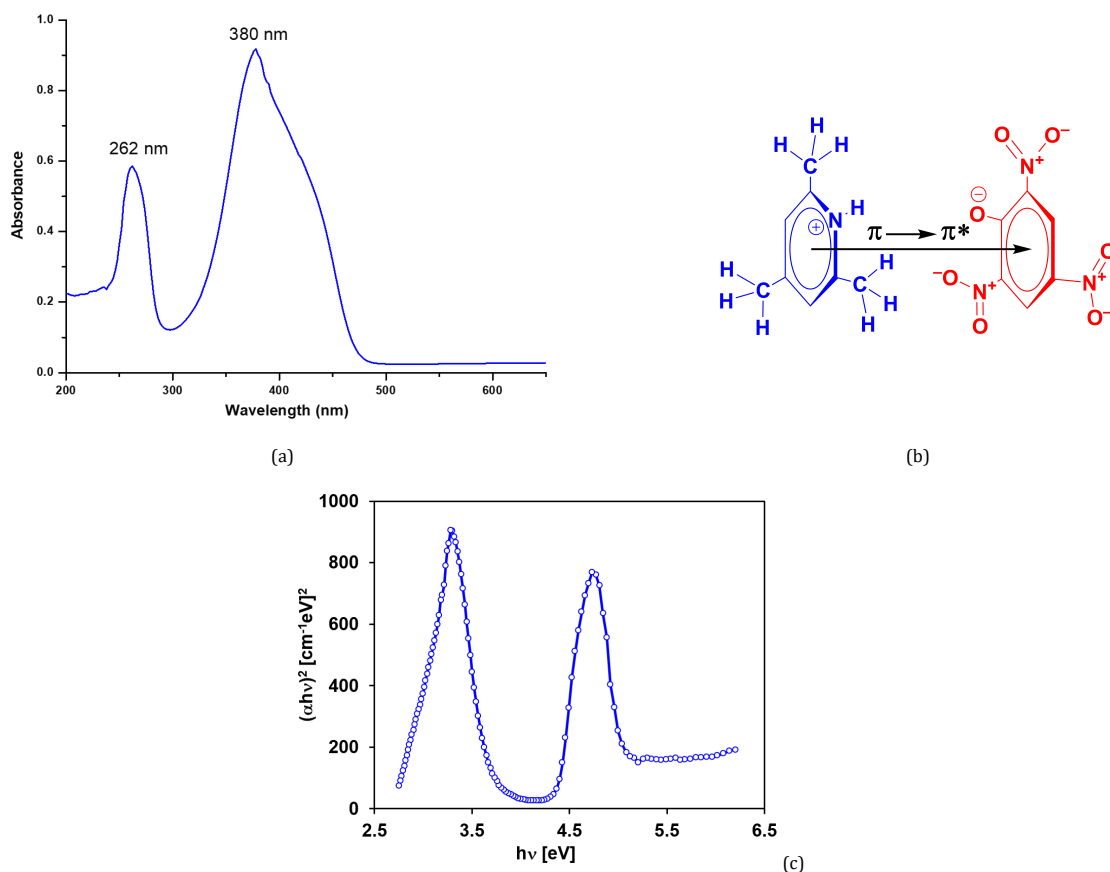


Figure 5. (a) UV-Vis spectrum, (b) the scheme of charge transfers intermolecular for the $\pi \rightarrow \pi^*$ transitions and (c) Tauc's plot of the 2,4,6-trimethylpyridinium picrate.

The aromatic molecules containing nitro functional group show a strong band in the region $1570\text{--}1485\text{ cm}^{-1}$ and $1370\text{--}1320\text{ cm}^{-1}$ due to the NO_2 asymmetric and symmetric stretching vibrations, respectively [27]. In the title organic salt, the sharp bands appearing at 1361 , 1329 cm^{-1} and 1347 , 1314 cm^{-1} in FT-IR and Raman spectra are assigned to the asymmetric and symmetric stretching vibrations of the NO_2 group of the picrate anions, respectively.

Other characteristics are observed at 868 , 787 , and 741 cm^{-1} in the FT-IR spectra and at 825 , 763 , and 719 cm^{-1} in the Raman spectra, which are caused by out-of-plane bending ($-\text{NO}_2$), in scissoring ($-\text{NO}_2$) vibration mode of the nitro groups, respectively, and these assignments are very characteristic of the picrate anion [28].

3.4. UV-Vis spectra and energy band gap

The UV-Vis spectrum of the 2,4,6-trimethylpyridinium picrate (Figure 5a) showed an absorption maximum at 262 nm due to its charge transfer intermolecular $\pi \rightarrow \pi^*$ transitions (Figure 5b). The absorbance at 380 nm was assigned to the transitions that take place in the 2,4,6-trimethylpyridine and picric acid moiety due to the shift of electrons from the non-bonding orbital to the anti-bonding orbital ($n \rightarrow \pi^*$). The optical band gaps (E_g) of 2,4,6-trimethylpyridinium picrate were calculated using Tauc's plot [29]. The optical band gaps were found by extrapolating the curve $(\alpha \times h\nu)^2 = 0$ (Inset of Figure 5c) and the obtained values are 2.7 and 4.3 eV , respectively. All this evidence supports the suggested structure and characteristic features of 2,4,6-trimethylpyridinium picrate.

3.5. HOMO and LUMO analysis

The frontier molecular orbitals (FOMs) of a molecule are the highest occupied molecular orbital (HOMO) and the lowest unoccupied molecular orbital (LUMO). Molecular orbitals and their properties like energy are very useful in understanding and interpreting nature. Their frontier electron density is used to predict the most reactive position in the π -electron system and explains several types of reactions in conjugated systems [30]. The electronic absorption corresponding to the transition from the ground state to the first excited state is mainly described by electron excitation from the HOMO to the LUMO. Moreover, the Eigenvalues of HOMOs (π -donor) and LUMOs (π -acceptor) and their energy gaps show the charge transfer interaction taking place within the molecule and reflect the chemical activity [31].

Theoretical structural studies were carried out for the title crystal by optimizing the structure in the gas phase using B3LYP functional with 6-311G(d,p) basis set. The electronic properties of the molecule are characterized by the analysis of the frontier orbitals. The energy values of the HOMO and HOMO-1, LUMO and LUMO+1 frontier molecular orbitals with the corresponding $\Delta E_{\text{HOMO-LUMO}}$ relative energy gap is shown in Figure 6. The positive and negative phase are represented in red and green color, respectively. As can be seen in Figure 6, the plot reveals that HOMO is primarily composed of the trinitrophenyl moiety corresponding to the benzene ring whereas the LUMO is spread over to the pyridinyl moiety of the molecule. The orbital energy level analysis for the title compound showed that HOMO and HOMO-1 values are -6.44 and -7.25 eV , while the values of LUMO and LUMO+1 are -2.73 and -2.58 eV , respectively.

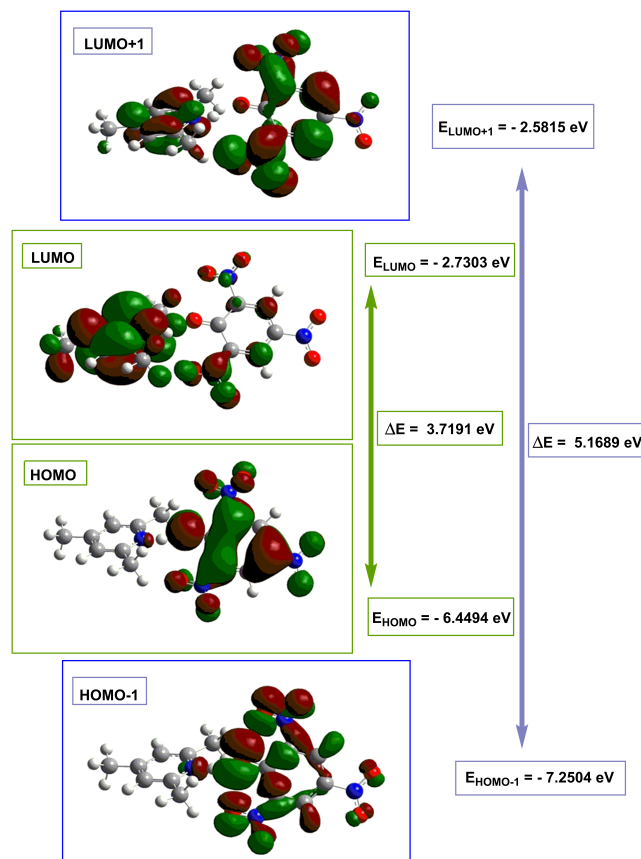


Figure 6. Frontier molecular orbital diagram for 2,4,6-trimethylpyridinium picrate.

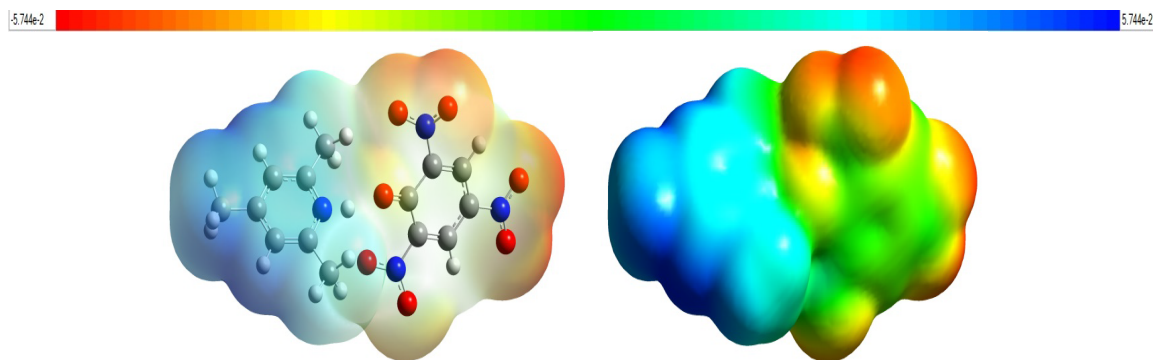


Figure 7. Molecular electrostatic potential map calculated at B3LYP/6-311G(d,p) level for the 2,4,6-trimethylpyridinium picrate.

The energy gap values of the title compound calculated at the DFT level are 3.71 and 5.16 eV, respectively. It can be said that the title compound, which has large HOMO-LUMO gaps 3.71 and 5.16 eV, respectively, implies high kinetic stability and low chemical reactivity.

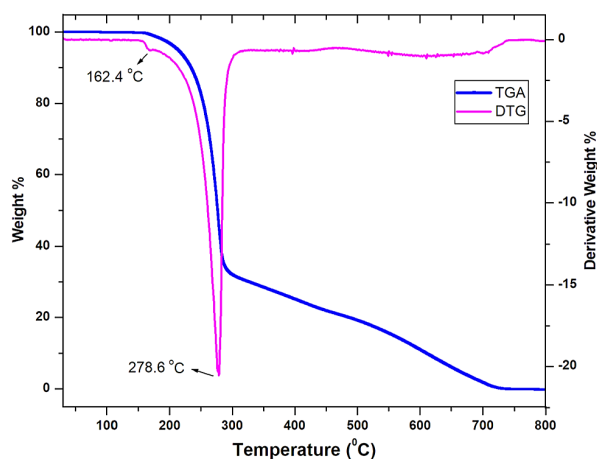
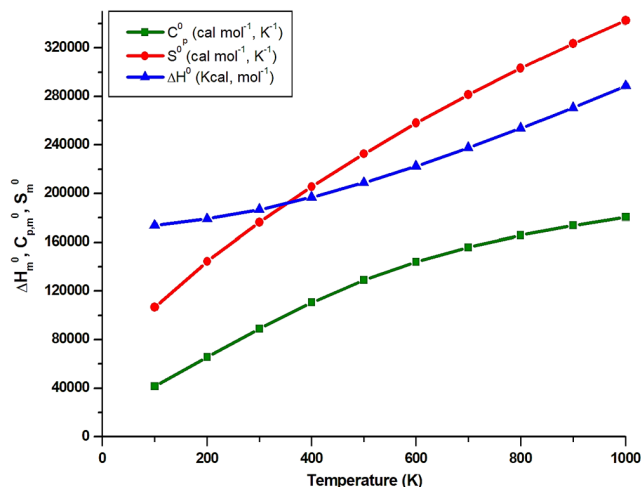
3.6. Molecular electrostatic potential (MEP)

The MEP is a colored plot mapped onto the isosurfaces of electron density, which can be experimentally measured with X-ray diffraction and calculated by using the B3LYP functional with 6-311G(d,p) basis set. The different values of the electrostatic potential on the surface are represented by different colors. Potential increases in order red < orange < yellow < green < blue. The color code of these maps is in the range between -5.744 a.u. (deepest red) and 5.744 a.u. (deepest blue) in the compound, where blue shows the strongest attraction

and red shows the strongest repulsion. Regions of negative $V(r)$ are usually associated with the lone pair of electronegative atoms [32]. To investigate the possible reactive sites of the structure to interact with the molecular electrostatic potential surface was generated [33]. It is known that nitro and methyl substituents in the aromatic ring have negative and positive inductive effects, respectively. As can be seen from the MEP map of the 2,4,6-trimethylpyridinium picrate compound (Figure 7), while the regions having the negative potential are over the electronegative atoms (oxygen atoms in the 2,4,6-trinitrophenyl ring), the regions having the positive potential are over the 2,4,6-trimethylpyridine ring. Consistent with the above results, the α -methyl, nitro, and amine parts play a crucial role in the chemical and intermolecular interactions.

Table 4. The calculated molecular electronic properties of the 2,4,6-trimethylpyridinium picrate (vacuum).

Parameters	Value
E_{HOMO} (eV)	-6.4494
E_{LUMO} (eV)	-2.7303
Energy band gap, $\Delta E = E_{\text{HOMO}} - E_{\text{LUMO}}$ (eV)	-3.7191
Ionization energy, $I = -E_{\text{HOMO}}$ (eV)	+6.4494
Electron affinity, $A = -E_{\text{LUMO}}$ (eV)	+2.7303
Chemical hardness, $\eta = (I-A)/2$ (eV)	1.8596
Chemical softness, $\zeta = 1/2\eta$ (eV)	0.2688
Nucleophilicity, $\varepsilon = 1/\omega$ (eV)	0.1765
Chemical potential, $\mu = -(I+A)/2$ (eV)	-4.5898
Electrophilicity index, $\omega = (\mu^2/2\eta)$ (eV)	5.6646
Electronegativity, $\chi = (I+A)/2$ (eV)	4.5898
Dipol moment (Debye)	15.4277
Electronic energy (a.u.)	-1287.5674

**Figure 8.** TGA-DTG thermograms of 2,4,6-trimethylpyridinium picrate.**Figure 9.** Thermodynamic properties of the 2,4,6-trimethylpyridinium picrate at different temperatures at B3LYP/6-311G(d,p) level.

The ionization energy (I), chemical potential (μ), hardness (η), softness (S), electronegativity (χ), and electrophilicity index (ω) of the molecule are calculated and depicted in Table 4.

3.7. Thermal properties

The thermal stability of the 2,4,6-trimethylpyridinium picrate was studied in a nitrogen atmosphere from 30 to 800 °C at a heating rate of 10 °C/min and the obtained TG/DTG diagram is given in Figure 8. TG curve indicates that there was no weight loss from 30 to 162 °C for the 2,4,6-trimethylpyridinium picrate compound. The molecule is stable up to 160 °C. The first peak at 160 °C is assigned to the dehydration of hygroscopic water (about 2.4%). After the dehydration of hygroscopic

water, the 2,4,6-trimethylpyridinium picrate compound undergoes two stages of decomposition. The first decomposition starts at ca. 162 °C and ends at 278 °C with the loss of weight (63.65%). This major weight loss coincides exactly with the peak (278 °C) of the DTG curve. This may be due to the evolution of hydrocarbon gases followed by ring rupture. The second weight loss occurs between 278 and 738 °C in the TG curve. This may be due to the liberation of various gaseous like volatile substances, ammonia, and nitrogen dioxide gases [34]. After this temperature, the curve begins to flatten out and the crystal decomposes completely without any residue. The 2,4,6-trimethylpyridinium picrate is stable up to 162 °C and hence, this crystal can be used for several applications.

3.8. Thermodynamic properties

The statistically thermodynamic parameters, such as the standard heat capacity of constant pressure ($C_{p,m}^{\circ}$), the enthalpy (ΔH_m°), and the entropy (S_m°), were calculated using the B3LYP/6-311G(d,p) method in the ground state by increasing from 100 to 1000 K in the gas phase. Figure 9 shows that $C_{p,m}^{\circ}$, S_m° , and ΔH_m° of the title compound increase from 100 to 1000 K, which is caused by the rise of molecular vibration intensity with the increasing temperature [35].

Quadratic formulas were used to fit the correlation equations between different parameters, such as heat capacity, enthalpy, entropy, and temperature; R being the corresponding fitting factor for these thermodynamic parameters. The corresponding fitting equations for the title compound are as presented below:

$$C_{p,m}^{\circ} = 12.8958 + 0.2937 T - 1.2688 \times 10^{-4} T^2 \quad (R^2 = 0.9997) \quad (1)$$

$$S_m^{\circ} = 72.8082 + 0.3725 T - 1.0422 \times 10^{-4} T^2 \quad (R^2 = 0.9971) \quad (2)$$

$$\Delta H_m^{\circ} = 167.1457 + 0.0454 T + 7.7029 \times 10^{-5} T^2 \quad (R^2 = 0.9994) \quad (3)$$

4. Conclusions

The 2,4,6-trimethylpyridinium picrate crystal obtained from 2,4,6-trimethylpyridine and picric acid was magnified by the slow evaporation technique in THF solvent. When it was investigated by a single crystal X-ray diffraction study, the crystal structure of the 2,4,6-trimethylpyridinium picrate compound has the feature of monoclinic space group and was found to be similar to literature data. A N-H...O type intramolecular hydrogen bonding and a C-H...O intermolecular weak interaction were observed in the crystal packing. The FT-IR, ^1H NMR, and ^{13}C NMR spectroscopic analyses confirm the crystallinity and purity of the material. When the crystal of the 2,4,6-trimethylpyridinium picrate compound is examined by X-ray analysis and spectroscopic data, it confirms the formation of proton transfer from picric acid to 2,4,6-collidine. The FT-IR spectrum, especially the ν_{NH} stretching vibration at 3327 cm^{-1} , was substantial to the presence of functional groups. The theoretical values of the bond length and bond angle agree well with the experimental values. The FOMs, the molecular electrostatic potential and the global reactivity descriptors were also calculated by using DFT methods and discussed. The identified HOMO-LUMO energy gap was discovered to be 3.71 eV, which explains the kinetic stability of the molecule. The molecular electrostatic potential map showed that the electron density of the picrate anion moiety was higher than that of the 2,4,6-trimethylpyridinium moiety. It was also observed the rising of molecular vibration intensity with the increasing temperature. The TG/DTG analysis showed that the title crystal is stable under $162 \text{ }^{\circ}\text{C}$, and it starts to decompose without leaving residue.

Acknowledgements

This work was supported by the Scientific Research Coordination Unit of Çanakkale Onsekiz Mart University, Çanakkale, Turkey, (Project no: FYL-2016-672).

Supporting information

CCDC-1548802 contains the supplementary crystallographic data for this paper. These data can be obtained free of charge via www.ccdc.cam.ac.uk/data_request/cif, or by e-mailing data_request@ccdc.cam.ac.uk, or by contacting The Cambridge Crystallographic Data Centre, 12 Union Road, Cambridge CB2 1EZ, UK; fax: +44(0)1223-336033.

Disclosure statement

Conflict of interest: The authors declare that they have no conflict of interest.
Ethical approval: All ethical guidelines have been adhered.
Sample availability: Sample of the compound is available from the author.

CRedit authorship contribution statement

Conceptualization: Fatma Aydin, Nahide Burcu Arslan; Methodology: Fatma Aydin, Nahide Burcu Arslan; Software: Nahide Burcu Arslan; Synthesis - Characterization: Fatma Aydin; Validation: Fatma Aydin, Nahide Burcu Arslan; Formal Analysis: Fatma Aydin, Nahide Burcu Arslan; Investigation: Fatma Aydin, Nahide Burcu Arslan; Data Curation: Fatma Aydin, Nahide Burcu Arslan; Writing - Original Draft: Fatma Aydin, Nahide Burcu Arslan; Writing - Review and Editing: Fatma Aydin, Nahide Burcu Arslan; Visualization: Fatma Aydin, Nahide Burcu Arslan; Funding acquisition: Fatma Aydin.

ORCID and Email

Nahide Burcu Arslan

burcu.aslan@giresun.edu.tr

<https://orcid.org/0000-0002-1880-1047>

Fatma Aydin

faydin@comu.edu.tr

<https://orcid.org/0000-0002-7219-6407>

References

- Sherman, A. R. 2,4,6-Collidine. *Encyclopedia of Reagents for Organic Synthesis* **2001**.
- Herzog, A.; Roesky, H. W.; Jäger, F.; Steiner, A. 2,4,6-Trimethylpyridine-bis(hydro)fluoride: a novel fluorinating reagent for organo transition-metal alkyls. *Chem. Commun. (Camb.)* **1996**, 29–30.
- Xue, X.-S.; Wang, Y.; Li, M.; Cheng, J.-P. Comprehensive energetic scale for quantitatively estimating the fluorinating potential of N-F reagents in electrophilic fluorinations. *J. Org. Chem.* **2016**, *81*, 4280–4289.
- Rozatian, N.; Ashworth, I. W.; Sandford, G.; Hodgson, D. R. W. A quantitative reactivity scale for electrophilic fluorinating reagents. *Chem. Sci.* **2018**, *9*, 8692–8702.
- André, V.; Lahrache, H.; Robin, S.; Rousseau, G. Reaction of unsaturated phosphonate monoesters with bromo- and iodo(bis-collidine) hexafluorophosphates. *Tetrahedron* **2007**, *63*, 10059–10066.
- CRC handbook of chemistry and physics*; Haynes, W. M., Ed.; 95th ed.; CRC Press: London, England, 2014.
- Handbook of reagents for organic synthesis: Acidic and basic reagents*; Reich, H. J.; Rigby, J. H., Eds.; John Wiley & Sons: Chichester, England, 1999.
- Aditya Prasad, A.; Muthu, K.; Rajasekar, M.; Meenatchi, V.; Meenakshisundaram, S. P. Synthesis, crystal growth, characterization and theoretical studies of 4-aminobenzophenonium picrate. *Spectrochim. Acta A Mol. Biomol. Spectrosc.* **2015**, *135*, 46–54.
- Dhanabal, T.; Amirthaganesan, G.; Dhandapani, M.; Das, S. K. Synthesis, structure, thermal and NLO characterization of 4-hydroxy tetramethylpiperazinium picrate crystals. *J. Chem. Sci. (Bangalore)* **2012**, *124*, 951–961.
- Chandramohan, A.; Bharathikannan, R.; Chandrasekaran, J.; Maadeswaran, P.; Renganathan, R.; Kandavelu, V. Synthesis, crystal growth and characterization of a new organic NLO material: Caffeinium picrate (CAFP)—A charge transfer molecular complex salt. *J. Cryst. Growth* **2008**, *310*, 5409–5415.
- Sudharsana, N.; Muthunatesan, S.; Jasmine Priya, G.; Krishnakumar, V.; Nagalakshmi, R. Experimental and theoretical studies of 2,5-dichloroanilinium picrate. *Spectrochim. Acta A Mol. Biomol. Spectrosc.* **2014**, *121*, 53–62.
- Chandramohan, A.; Bharathikannan, R.; Kandavelu, V.; Chandrasekaran, J.; Kandhaswamy, M. A. Synthesis, crystal growth, structural, thermal and optical properties of naphthalene picrate an organic NLO material. *Spectrochim. Acta A Mol. Biomol. Spectrosc.* **2008**, *71*, 755–759.
- Hankin, S. M.; John, P.; Smith, G. P. Laser time-of-flight mass spectrometry of PAH–Picrate complexes. *Anal. Chem.* **1997**, *69*, 2927–2930.
- Koizumi, S.; Matsunaga, Y. The phenanthrene/anthracene–picric acid system. *Bull. Chem. Soc. Jpn.* **1974**, *47*, 9–13.
- Akhavan, J. *The chemistry of explosives*; Royal Society of Chemistry: Cambridge, England, 1998.
- Peng, Y.; Zhang, A.-J.; Dong, M.; Wang, Y.-W. A colorimetric and fluorescent chemosensor for the detection of an explosive—2,4,6-trinitrophenol (TNP). *Chem. Commun. (Camb.)* **2011**, *47*, 4505.

- [17]. Schechter, B.; Arnon, R.; Freedman, Y.; Chen, L.; Wilchek, M. Liver accumulation of TNP-modified streptavidin and avidin: Potential use for targeted radio- and chemotherapy. *J. Drug Target.* **1996**, *4*, 171–179.
- [18]. Stilić, V.; Kaitner, B. Hydrogen bonding in pyridinium picrates: From discrete ion pairs to 3D networks. *Cryst. Growth Des.* **2011**, *11*, 4110–4119.
- [19]. Bruker (2008). SHELXL-97. Bruker AXS Inc., Madison, Wisconsin, USA.
- [20]. Bruker (1997). SHELXS-97. Bruker AXS Inc., Madison, Wisconsin, USA.
- [21]. Frisch, M. J.; Trucks, G. W.; Schlegel, H. B.; Scuseria, G. E.; Robb, M. A.; Cheeseman, J. R.; Montgomery, J. A.; Vreven, T.; Kudin, K. N.; Burant, J. C.; Millam, J. M.; Iyengar, S. S.; Tomasi, J.; Barone, V.; Mennucci, B.; Cossi, M.; Scalmani, G.; Rega, N.; Petersson, G. A.; Nakatsuji, H.; Hada, M.; Ehara, M.; Toyota, K.; Fukuda, R.; Hasegawa, J.; Ishida, M.; Nakajima, T.; Honda, Y.; Kitao, O.; Nakai, H.; Klene, M.; Li, X.; Knox, J. E.; Hratchian, H. P.; Cross, J. B.; Adamo, C.; Jaramillo, J.; Gomperts, R.; Stratmann, R. E.; Yazyev, O.; Austin, A. J.; Cammi, R.; Pomelli, C.; Ochterski, J. W.; Ayala, P. Y.; Morokuma, K.; Voth, G. A.; Salvador, P.; Dannenberg, J. J.; Zakrzewski, V. G.; Dapprich, S.; Daniels, A. D.; Strain, M. C.; Farkas, O.; Malick, D. K.; Rabuck, A. D.; Raghavachari, K.; Foresman, J. B.; Ortiz, J. V.; Cui, Q.; Baboul, A. G.; Clifford, S.; Cioslowski, J.; Stefanov, B. B.; Liu, G.; Liashenko, A.; Piskorz, P.; Komaromi, I.; Martin, R. L.; Fox, D. J.; Keith, T.; Al-Laham, M. A.; Peng, C. Y.; Nanayakkara, A.; Challacombe, M.; Gill, P. M. W.; Johnson, B.; Chen, W.; Wong, M. W.; Gonzalez, C.; Pople, J. A. Gaussian 09, Revision E.01, Gaussian, Inc., Wallingford CT, **2009**.
- [22]. Aditya Prasad, A.; Muthu, K.; Rajasekar, M.; Meenatchi, V.; Meenakshisundaram, S. P. Crystal growth, characterization and theoretical studies of 4-aminopyridinium picrate. *Spectrochim. Acta A Mol. Biomol. Spectrosc.* **2015**, *135*, 805–813.
- [23]. Srivastava, K. K.; Shubha, S.; Tanweer, A.; Rituraj An Overview of Picric Acid. *Der Pharma Chemica* **2017**, *9*, 64–75.
- [24]. Coates, J. Interpretation of infrared spectra, A practical approach. *Encyclopedia of Analytical Chemistry* **2006**.
- [25]. Smith, B. C. *Infrared spectral interpretation: A systematic approach*; CRC Press: Boca Raton, FL, 1998.
- [26]. Hendra, P.; etc.; Jones, C.; Warnes, G. *Fourier transform Raman spectroscopy: Instrumental and chemical applications*; Ellis Horwood Ltd, Publisher: Harlow, England, 1991.
- [27]. Clarkson, J.; Smith, W. E.; Batchelder, D. N.; Smith, D. A.; Coats, A. M. A theoretical study of the structure and vibrations of 2,4,6-trinitrotoluene. *J. Mol. Struct.* **2003**, *648*, 203–214.
- [28]. Aydin, F.; Arslan, N. B. Synthesis, spectral properties, crystal structure and theoretical calculations of a new geminal diamine: 2,2,2-Trichloro-N,N'-bis(2-nitrophenyl)-ethane-1,1-diamine. *J. Mol. Struct.* **2021**, *1232*, 129976.
- [29]. Tauc, J.; Grigorovici, R.; Vancu, A. Optical properties and electronic structure of amorphous germanium. *Phys. Status Solidi B Basic Res.* **1966**, *15*, 627–637.
- [30]. Fukui, K.; Yonezawa, T.; Shingu, H. A molecular orbital theory of reactivity in aromatic hydrocarbons. *J. Chem. Phys.* **1952**, *20*, 722–725.
- [31]. Parr, R. G.; Szentpály, L. v.; Liu, S. Electrophilicity index. *J. Am. Chem. Soc.* **1999**, *121*, 1922–1924.
- [32]. Murray, J. S. *Molecular electrostatic potentials: Concepts and applications*; Murray, J. S.; Sen, K., Eds.; Elsevier Science & Technology, 1996.
- [33]. Geerlings, P.; Proft, F. D.; Ayers, P. W. Chapter 1 Chemical reactivity and the shape function. In *Theoretical and Computational Chemistry*; Elsevier, 2007; pp. 1–17.
- [34]. Jauhar, R. O. M. U.; Viswanathan, V.; Vivek, P.; Vinitha, G.; Velmurugan, D.; Murugakoothan, P. A new organic NLO material isonicotinamidium picrate (ISPA): crystal structure, structural modeling and its physico-chemical properties. *RSC Adv.* **2016**, *6*, 57977–57985.
- [35]. Bevan Ott, J.; Boerio-Goates, J. *Chemical thermodynamics: Advanced applications: Advanced applications*; Academic Press: San Diego, CA, 2000.



Copyright © 2022 by Authors. This work is published and licensed by Atlanta Publishing House LLC, Atlanta, GA, USA. The full terms of this license are available at <http://www.eurjchem.com/index.php/eurjchem/pages/view/terms> and incorporate the Creative Commons Attribution-Non Commercial (CC BY NC) (International, v4.0) License (<http://creativecommons.org/licenses/by-nc/4.0>). By accessing the work, you hereby accept the Terms. This is an open access article distributed under the terms and conditions of the CC BY NC License, which permits unrestricted non-commercial use, distribution, and reproduction in any medium, provided the original work is properly cited without any further permission from Atlanta Publishing House LLC (European Journal of Chemistry). No use, distribution or reproduction is permitted which does not comply with these terms. Permissions for commercial use of this work beyond the scope of the License (<http://www.eurjchem.com/index.php/eurjchem/pages/view/terms>) are administered by Atlanta Publishing House LLC (European Journal of Chemistry).